Cytomechanical Properties of *Papaver* Pollen Tubes Are Altered after Self-Incompatibility Challenge

Anja Geitmann,*¶ William McConnaughey,† Ingeborg Lang-Pauluzzi,‡ Vernonica E. Franklin-Tong,§ and Anne Mie C. Emons¶

*Institut de Recherche en Biologie Végétale, Université de Montréal, Montreal, Quebec, Canada; †Department of Biological Chemistry, Washington University, School of Medicine, St. Louis, Missouri USA; ‡Department of Cell Physiology, University of Vienna, Vienna, Austria; §School of Biosciences, The University of Birmingham, Edgbaston, Birmingham, United Kingdom; and ¶Plant Cell Biology, Wageningen University, Wageningen, The Netherlands

ABSTRACT Self-incompatibility (SI) in *Papaver rhoeas* triggers a ligand-mediated signal transduction cascade, resulting in the inhibition of incompatible pollen tube growth. Using a cytomechanical approach we have demonstrated that dramatic changes to the mechanical properties of incompatible pollen tubes are stimulated by SI induction. Microindentation revealed that SI resulted in a reduction of cellular stiffness and an increase in cytoplasmic viscosity. Whereas the former cellular response is likely to be the result of a drop in cellular turgor, we hypothesize that the latter is caused by as yet unidentified cross-linking events. F-actin rearrangements, a characteristic phenomenon for SI challenge in *Papaver*, displayed a spatiotemporal gradient along the pollen tube; this suggests that signal propagation occurs in a basipetal direction. However, unexpectedly, local application of SI inducing S-protein did not reveal any evidence for localized signal perception in the apical or subapical regions of the pollen tube. To our knowledge this represents the first mechanospatial approach to study signal propagation and cellular responses in a well-characterized plant cell system. Our data provide the first evidence for mechanical changes induced in the cytoplasm of a plant cell stimulated by a defined ligand.

INTRODUCTION

Intracellular signal transduction and cellular responses are generally studied using biochemistry. However, cytomechanical investigations have recently provided another approach. Two facets of intracellular signaling are relevant to a mechanospatial approach. First, the question of how the signal and response propagate within the three-dimensional space of the cell, and second, what alterations in cytomechanical properties are stimulated.

External signals triggering intracellular signaling cascades are usually perceived by transmembrane receptors whose localization may be distributed all over the cell surface or in specific regions of the cell (see Loitto et al., 2001; Strutt, 2001, for examples). In both cases the signal must propagate through the lumen of the cell to elicit a response. Since the cell is a three-dimensional space with subcompartmentalization comprising organelles, the complexity of propagation in space within the cell is considerable. The concept of ''Ca^{2+} signatures'' has been developed to account for the huge range of responses that can be obtained from a simple signal that can vary almost infinitely in amplitude, time, and space, thereby allowing a specific response (Rudd and Franklin-Tong, 2001). To initially consider the signal propagation and the mechanical alterations stimulated in the cell, a simple model system would require a monodimensional rather than a bi- or tridimensional structure. In animal cells, neurons provide a quasimonodimensional system that has been studied in detail (Palanivelu and Preuss, 2000). A comparable plant cell system, the pollen tube, has similar monodimensional properties to neuronal cells. Pollen tubes are long, thin, tubular cells (Heslop-Harrison, 1987). On a subcellular scale, signal propagation can proceed in any direction between plasma membrane and cell lumen. However, on a larger, cellular scale, signal propagation can basically proceed in two opposite directions—acropetal or basipetal—to or from the apex of the tip growing cell.

The tubular and highly anisotropic geometry of the pollen tube is not only ideal for the investigation of signal propagation and transduction but also allows for relatively easy assessment and interpretation of certain mechanical aspects of the cellular response. The observation of intracellular movement is straightforward since bulk organelle movement takes place parallel to the longitudinal axis of the cell, thus reducing the degrees of freedom from nine (position, velocity, and acceleration in the x, y, and z directions in a three-dimensional space) to three (position, velocity, and acceleration in the x direction).

To understand the physical implications of the cellular response to a signal, the cell mechanical properties have to be taken into account. A living animal cell is often modeled as a continuum that contains an elastic cortex, comprising the plasma membrane and underlying cytoskeletal elements, that surrounds a viscous (Evans and Yeung, 1989) or viscoelastic (Schmid-Schoenbein et al., 1995) fluid (the cytoplasm). A more advanced model depicts the cell as a prestressed tensegrity structure (Ingber, 1993; Stamenovic et al., 1996; Stamenovic and Coughlin, 1999; Wang et al., 2001) that

Submitted September 10, 2003, and accepted for publication January 21, 2004.

Address reprint requests to Anja Geitmann, Institut de Recherche en Biologie Végétale, Université de Montréal, 4101 rue Sherbrooke est, Montréal, Québec H1X 2B2 Canada. Tel.: 514-872-8492; Fax: 514-872-9406; E-mail: anja.geitmann@umontreal.ca.

0006-3495/04/05/3314/10 $2.00

emphasizes the role of the cytoskeleton for cellular structure. In living plant cells the structural role of the cytoskeleton is still largely unknown, but it is likely to be much less significant than the forces governed by the cell wall and the turgor pressure (Lintilhac et al., 2000). In a simplified approach, a pollen tube can be modeled as a thin-walled, sausage-shaped pressure vessel that consists of a viscoelastic fluid (the cytoplasm structured by a network of cytoskeletal elements) confined by an elastic shell (the plasma membrane and the cell wall). Local deformation will cause the viscoelastic liquid to be displaced. The viscous component in the viscoelastic behavior can be determined by assessing the amount of hysteresis during relaxation after mechanical deformation. The simple, sausage-shaped geometry of pollen tubes facilitates the analysis of deformation experiments and has allowed us to obtain information on the physical state of the cytoplasm.

Here we present data relating to studies on mechanical aspects of signal transduction and cellular response in the in vitro-grown pollen tubes of *Papaver rhoeas* (the field poppy) undergoing the self-incompatibility (SI) response. SI is a genetically controlled system that prevents self-fertilization by an interaction between stigmatic S-proteins, which act as signaling ligands, and pollen tubes, in an S-allele-specific manner (Wheeler et al., 2001). This triggers the *S*-specific inhibition of incompatible pollen tube growth (Foote et al., 1994; Franklin-Tong et al., 1995). Previous studies have shown that the SI induction in incompatible *P. rhoeas* pollen tubes triggers an intracellular signaling cascade (Franklin-Tong et al., 1993, 1997; Rudd and Franklin-Tong, 2003), which may result in programmed cell death (Jordan et al., 2000; Rudd and Franklin-Tong, 2003; Geitmann et al., 2004). In a recent study we showed that alterations in the actin cytoskeleton represent an important component in the SI response in *P. rhoeas* pollen tubes. These comprise dramatic rearrangements in the filamentous (F-)actin configuration, initiating within a few seconds, and are accompanied by F-actin depolymerization (Geitmann et al., 2000, 2001; Snowman et al., 2002). The alterations follow a clearly identified temporal pattern:

1. Loss of the apical actin mesh (within 1 min).
2. Increase of F-actin at the cell periphery (within 1–2 min).
3. Disintegration of actin bundles and appearance of a fine-speckled pattern (within 5–10 min).
4. Formation of punctate foci (within 20 min) (Geitmann et al., 2000).

These alterations in the actin configuration are likely to impact on the overall mechanical properties of the cell since the cytoskeleton is considered to play a major role in converting biochemical reactions into mechanical forces (Baluska et al., 2000; Vidali and Hepler, 2001; Vantard and Blanchoin, 2002).

Here we have investigated some aspects of the mechanical and spatial alterations induced by the SI response in *P. rhoeas* pollen tubes, and attempt to relate these to the changes in the actin cytoskeleton stimulated by this response. We compared the mechanical properties of normally growing pollen tubes and those in which SI was induced. Our data demonstrate that dramatic changes to the mechanical properties of the pollen tubes are stimulated by the SI response. We also show that cellular responses are propagated in a basipetal direction in *P. rhoeas* pollen tubes. Unexpectedly, we found no evidence for a localization of signal perception in the apical or subapical parts of the pollen tube. Our data provide the first evidence for mechanical changes induced in the cytoplasm of a plant cell stimulated by a defined ligand.

MATERIALS AND METHODS

Plant material

Plants of *Papaver rhoeas* L. (Shirley variety) segregating for known self-incompatibility genotypes (*S1S1*, *S1S3*, *S2S4*, and *S4S6*) were used for the experiments involving S-proteins (see Franklin-Tong et al., 1988). Pollen was stored at −20°C over silica gel until required.

In vitro growth of pollen tubes

Pollen was grown as described in Geitmann et al. (2000). For micro-indentation experiments, pollen was grown on coverslips coated with poly-L-lysine and covered with liquid growth medium (GM). For drug-induced depolymerization of actin filaments, cytochalasin D, latrunculin A, or latrunculin B (Sigma, St. Louis, MO) were prepared from stock solutions and diluted in GM. Unless noted otherwise, concentrations previously established to cause breakdown of filamentous actin in pollen tubes were used: 1 μM for cytochalasin D, 50 nM for latrunculin A, and 200 nM for latrunculin B.

Production of recombinant S-protein in *Escherichia coli*

Recombinant S-proteins S_1e and S_3e were prepared as described in Kakeda et al. (1998). The purified proteins were kept at −70°C and dialyzed overnight against GM before use. Dialyzed S-proteins were kept at 4°C. The concentrations of S-proteins after dialysis was determined with the protein assay kit BCA-200 (Pierce, Rockford, IL).

Self-incompatibility challenges of in vitro growing pollen tubes

Pollen from plants of *S* genotype *S1S3* or *S1S1* (incompatible) and *S2S4* or *S4S6* (fully compatible) were grown on an agarose-GM layer and covered with liquid GM as described. SI was induced by replacing the layer of liquid GM with GM containing recombinant S-proteins S1e (20 μg mL^{-1}) and/or S3e (30 μg mL^{-1}) (Geitmann et al., 2000).

Fluorescence microscopy

Pollen tubes were treated with freshly prepared *m*-maleimidobenzoyl *N*-hydroxysuccinimide ester at 100 μM (Sigma-Aldrich Chemie BV, Zwijndrecht, The Netherlands) in GM for 5 min. They were subsequently fixed and treated as described in Geitmann et al. (2000).

Fluorescence microscopy was performed with a Nikon Microphot-FXA (Surrey, UK) equipped with a Nikon PlanApo ×60 oil immersion objective (NA 1.40) and a Photometrics Quantix cooled charge-coupled device camera (Roper Scientific, Trenton, NJ). Standard filter sets for fluorescein isothiocyanate were used. Data were processed with IPLab Spectrum software (Scanalytics, Fairfax, VA) and Photoshop (Adobe Systems, San Jose, CA).

UV microscopy

UV microscopy was performed using a Zeiss ACM microscope equipped for UV light. The microscope is equipped with a monochromator and operated either with a Hg or a Xe lamp. A 0.8 ultrafluor condensor was used in combination with ultrafluar glycerol immersion lenses (32× 0.40 NA; 100× 1.25 NA). Images were captured with a Bosch UV sensitive camera and processed with a Hamamatsu DVS-3000. Videos were recorded with an Umatic Hi Band recorder (Sony, San Diego, CA). Observations were performed at a wavelength of 440 nm which had been shown not to be harmful to pollen tube growth within the observation period of 60 min (data not shown).

Microindentation

The design and principles of operation of the microindenter have been described previously (Petersen et al., 1982; Elson et al., 1983). Briefly, the bending of a horizontal glass beam gauges the resistance to cellular deformation performed by a vertical glass stylus attached to one end of the beam. The other end of the beam is mounted on a linear piezoelectric motor which moves vertically according to a programmed waveform. Optical sensors monitor the vertical positions of the stylus and the motor. The extent to which the beam is bent is proportional to the force exerted on the stylus by the cell and is determined by comparing stylus displacements in the presence and absence of cell contact. The force exerted by the cell on the stylus is determined with the help of the force constant of the beam, which is obtained by prior calibration. The microindentation assembly used here was mounted on a Zeiss IM 35 inverted light microscope. In the experiments reported in this article, the vertical glass stylus had a tip diameter of 4 μm and the motor was programmed to execute a single triangular waveform with a velocity of 4 $\mu m/s^{-1}$ and a total amplitude of 10 μm. This implies that the stylus started moving through medium before touching the object. This elevated position of the stylus allowed for quick change of position, thus reducing time delay between measurements. Furthermore, the path taken by the stylus through the medium before touching the object helped us to assess whether vibrations disturbed the measurement and whether the stylus was shifted during the process. The path through the medium did not contribute any other information, however, and therefore only 1 μm of it was included in the force distance graphs. The deformation force was measured in mdyn/μm^{-1} since we considered the pollen tube to react as an elastic spring (and/or a dashpot). We thus ignored the three-dimensional geometry of the stylus-pollen tube interaction which was not a variable in our set up, since neither the shape of the pollen tube nor the shape of the stylus varied between experiments.

Except for the apical 20 μm and regions containing large vacuoles or the male germ unit, pollen tubes show rather uniform stiffness along the tube (Geitmann and Parre, 2004; A. Geitmann, unpublished results). To avoid the regions showing irregularities, deformations analyzed here were performed at 40 ± 10 μm from the pollen tube apex.

Local application of S-protein

S_1e-protein (20 $\mu g\ mL^{-1}$) in GM was applied to *S1S1* pollen tubes growing on the surface of an agarose layer using a micropipette as described for root hairs in Esseling et al. (2003). Volumes of 0.01–0.1 pl were applied to the cell surface at the apex, subapex, or distal region of the cell and subsequently pollen tube growth and cytoplasmic streaming were assessed to determine the presence of SI induction.

RESULTS

Organelle distribution and dynamics are altered by the SI response

In previous studies we showed that the SI response stimulates F-actin to undergo major changes that involve actin depolymerization (Geitmann et al., 2000; Snowman et al., 2002). As F-actin is the major structural element supporting long-distance organelle transport in pollen tubes, we investigated alterations to organelle distribution and dynamics stimulated by SI. Observation of normally growing pollen tubes revealed rapid organelle movement parallel to the longitudinal axis of the cell. For convenience we distinguish three different parts of the pollen tube in this article, namely the apex (apical 20 μm of the tube characterized by fine actin mesh), the subapical region (shank region of the tube between 20 and 100 μm from the apex), and the distal regions (shank regions further distal than 100 μm from the apex). Both subapical and distal regions are characterized by thick, longitudinally arranged bundles of actin filaments that are responsible for bulk organelle transport. In these regions, large organelles and smaller vesicles were rapidly transported toward the growing apex. In the apical area 10–20 μm from the apex, movement of the larger organelles slowed down slightly, before they were transported back in a basipetal direction resuming the same speed as before. Small vesicles crossed this area and accumulated in the apex where they could not be distinguished clearly due to their small size (Figs. 1 *A* and 2 *D*). However, their rapid vibrational displacements resembled Brownian movement.

After an incompatible SI challenge cytoplasmic streaming was arrested; the phenomenon resembled particle movement in a liquid that undergoes an enormous increase in viscosity. Pollen tube growth was arrested ~10–120 s after addition of S-protein and bulk organelle movement slowed down gradually starting a few minutes later. Five to twenty minutes after SI challenge organelles abandoned any kind of movement; not even vibrational movement could be observed ($n = 24$). Within an individual pollen tube, the arrest of cytoplasmic streaming in distal regions occurred later than in subapical parts of the cell. However, eventually movement stopped in all parts of the pollen tube. As a result, the SI-challenged cell looked very similar to one that had been treated with chemical fixation agents. It was notable that the characteristic distribution of organelles was not disturbed during this process, since the vesicle-rich clear zone in the apical dome remained clear; no bigger organelles entered this area (Fig. 1, *B–D*). No effect on pollen tube growth and cytoplasmic streaming was observed upon addition of S-protein to compatible pollen tubes ($n = 7$).

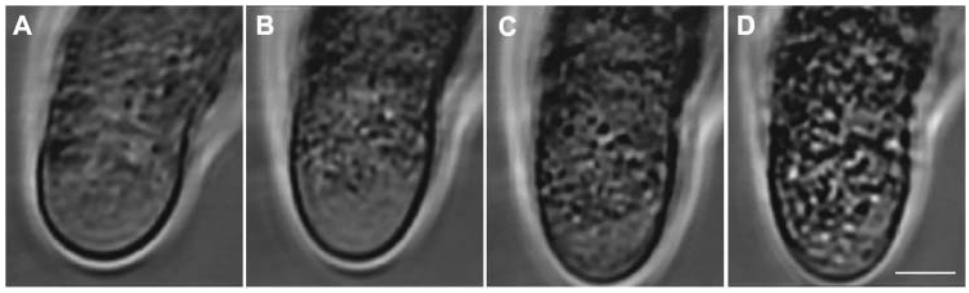

FIGURE 1 Cytoarchitecture is maintained after treatment with incompatible S-protein. Time lapse images of the apical region of one pollen tube 1, 4, 6, and 8 min after S-protein challenge. Observations made in the UV microscope. Bar = 3 μm. (*A*) At 1 min, growth had arrested but the cytoarchitecture appeared identical to that of unchallenged pollen tubes (compare with Fig. 2 *D*). (*B*) At 4 min, organelle movement had slowed down considerably in this region. (*C*) At 6 min organelle movement was completely arrested. (*D*) The clear zone in the apical dome remained devoid of larger organelles albeit becoming more contrast-rich at 8 min due to a general increase in granular structure of the cytoplasm. The apparent reduction in the size of the clear zone at later times was due to the entire cell assuming a more granular and contrast rich appearance in the light microscope.

As we postulated that actin depolymerization might play a role in these cytoplasmic alterations, we tested the effect of actin depolymerizing drugs. They rapidly destroyed the well-organized cytoarchitecture characteristic of a typical growing pollen tube. Treatment with cytochalasin D ($n = 5$), latrunculin A ($n = 6$), or latrunculin B ($n = 3$) resulted in larger organelles entering the clear zone at the apex of the tube within minutes after drug addition (Fig. 2). In contrast to SI-induced pollen tubes, although cytoplasmic streaming was arrested after drug addition, the organelles continued to oscillate rapidly and erratically in what resembled Brownian movement; this vibrational activity was still present at least 40 min after drug treatment.

SI stimulates changes to the physical state of the cytoplasm

The observation of complete arrest of organelle movement in SI-challenged pollen tubes led us to postulate that an increase in cytoplasmic viscosity might be involved as an SI response. To further test this hypothesis, we performed mechanical deformation experiments using microindentation (see Materials and Methods) and measured the stiffness and degree of viscosity of normally growing and SI-challenged pollen tubes. In normally growing pollen tubes, with the exception of regions that contained large vacuoles or the male germ unit, the viscosity of the cytoplasm within the ''shank'' of individual pollen tubes generally did not vary significantly, whereas stiffness showed the tendency to increase very slightly with a slope of 0.52 $\pm$ 0.62 mdyn/μm^{-2} along its length in the region between 20 and 80 μm from the apex ($n = 13$ pollen tubes). The shank region of an unchallenged, normally growing pollen tube reacted to deformation in a manner similar to an ideal spring. A typical force-distance graph is shown in Fig. 3 *A*. The stiffness of the deformed cell was obtained by calculating the slope of the force-distance graph. At a distance of 40 $\pm$ 10 μm from the apex the mean stiffness of a growing *P. rhoeas* pollen tube was 305.0 $\pm$ 91.7 mdyn/μm^{-1} ($n = 17$ pollen tubes; $n = 78$ measurements). Generally, the deformation was linear and no significant hysteresis was observed upon retraction of the glass stylus. This is consistent with the observation that the cytoplasm of normally growing pollen tubes has a low degree of viscosity and that the tube is under turgor pressure.

Fig. 3 *B* represents a typical example that demonstrates delayed elastic recovery after deformation. A large degree of hysteresis upon indenter retraction was observed. This phenomenon was typical for pollen tubes that had been treated with S-protein 20–120 min previously ($n = 14$ pollen tubes). It would have been desirable to assess these physical parameters immediately after SI challenge, but the experimental set up of the microindentation device has prevented us so far from obtaining data at time points earlier than 20 min after SI induction. The reason was that flooding

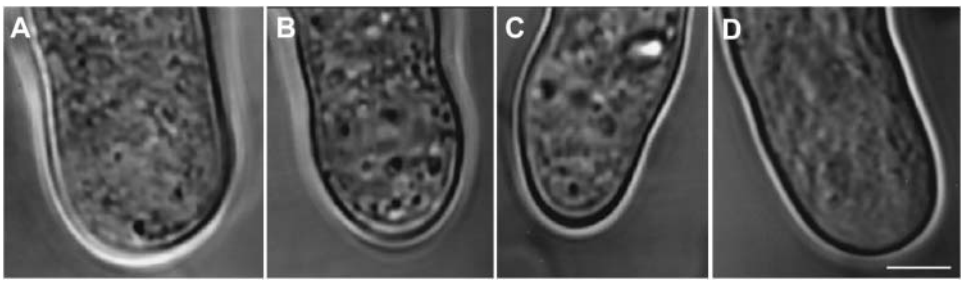

FIGURE 2 Cytoarchitecture is rapidly disturbed after treatment with actin depolymerizing drugs. Pollen tubes after 1 μM cytochalasin D (*A*), after 10 μM cytochalasin D (*B*), after 200 nM latrunculin B (*C*), and after exchange of medium (control) (*D*). Bigger organelles rapidly entered the clear zone and thus destroyed the cytoarchitecture in pollen tubes treated with actin depolymerizing drugs. Organelles kept vibrating for at least 40 min after treatment. The control pollen tube shows a smooth structure of the cytoplasm in the apical dome indicating an intact clear zone. Bar = 3 μm.

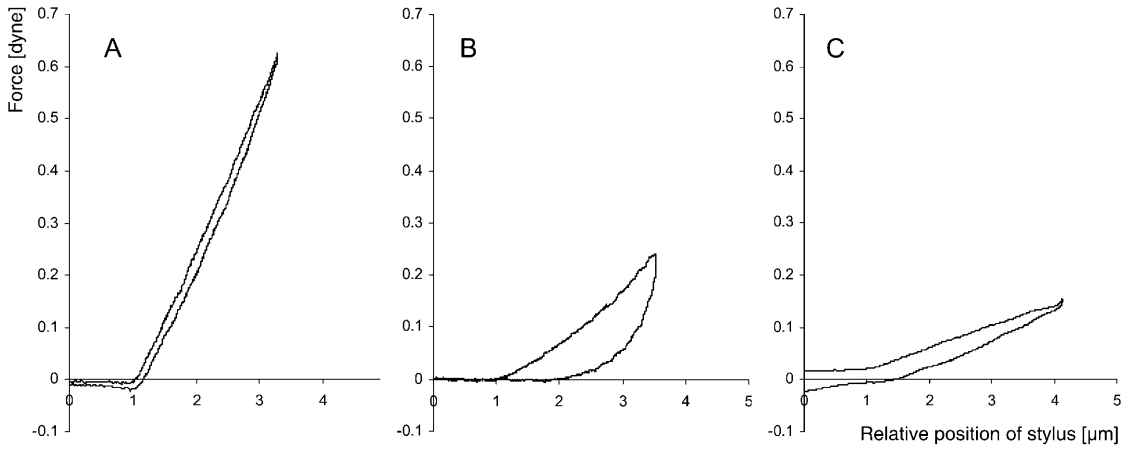

FIGURE 3 Cellular stiffness and viscoelasticity change after S-protein treatment. Force-distance graph of the local deformation of pollen tubes in the region 40 ± 10 μm behind the apex. The indenter moves through liquid medium (the last μm before contact is included in the graph) and then touches the pollen tube surface. Indentation speed is 4 $\mu m/s^{-1}$. (*A*) Normally growing Papaver pollen tube. The deformation is fully elastic since down- and upward movement follow almost identical paths. (*B*) Effect of self-incompatibility challenge. Papaver pollen tube 29 min after addition of S-protein to the medium. The slope of the deformation is lower, indicating reduced stiffness. It also shows considerable hysteresis upon retraction of the indenter, expressed by the large surface area between the two curves for down- and upward movement. (*C*) Effect of untriggered growth arrest. Papaver pollen tube that has seized elongating without external trigger. The slope of the deformation is lower, indicating reduced stiffness, which is consistent with a reduced turgor. Typically, no or only slight delay of elastic recovery appeared upon retraction of the stylus.

experiments would have necessitated quantities of S-protein that were unavailable to us (5 ml S-protein solution in the appropriate concentration per experiment). We therefore developed an alternative method in which small drops of S-protein solution were used to cover the pollen tubes before submerging the slides into the experimental chamber filled with pure GM. This method involved a time delay between SI challenge and measurement, however, since the SI reaction was reversible during the first minutes and since the microindenter had to be adjusted after placing the specimen. As a result we were not able to monitor a time course of the changes in stiffness and viscosity, but instead we assessed the final state. At this point of time in the SI reaction, a number of protein phosphorylation processes were taking place in the cytoplasm (Franklin-Tong et al., 1993, 1997; Rudd and Franklin-Tong, 2003) that later in the process led to an apoptotic demise of the cell (Jordan et al., 2000; Rudd and Franklin-Tong, 2003; Geitmann et al., 2004).

In addition to the increase in hysteresis in SI-challenged pollen tubes, the stiffness at 40 ± 10 μm behind the tip of the SI-challenged pollen tube was reduced to 92.4 ± 39.8 mdyn/μm^{-1} ($n = 6$ pollen tubes, $n = 11$ measurements). This represents a significant 3.3-fold change in the stiffness of the cell ($p < 0.001$). We hypothesized that the decrease in stiffness is caused by a decrease of the turgor pressure in the challenged cell whereas the delay in elastic recovery implies that the cytoplasm had assumed a higher viscosity. To show that the increase in hysteresis is indeed independent of the decrease in turgor we assessed the stiffness and hysteresis in pollen tubes that had arrested growth and thus were likely to show reduced turgor. Fig. 3 *C* shows that stiffness in these tubes was indeed reduced, whereas hysteresis was not increased or only slightly increased. Similar results were observed in pollen tubes subjected to flooding with hyperosmotic medium (A. Geitmann, unpublished results).

Spatial gradient of arrest of cytoplasmic streaming and actin rearrangement

Our observations on cytoplasmic streaming revealed that the time interval between challenge and arrest of organelle movement varied depending on the distance of the observed part of the cell from the pollen tube apex. This suggested that the arrest of cytoplasmic streaming propagated from one end of the cell to the other, starting at the apex or in the apical region. We investigated the speed of this propagation. Fig. 4 *A* illustrates that a clear spatial gradient relating to the arrest of cytoplasmic streaming was present between the apical and distal parts of the pollen tube. Total arrest of cytoplasmic streaming propagated with a mean speed of 55 $\mu m/min^{-1}$ ($n = 11$) within the pollen tube. In contrast, arrest of cytoplasmic streaming after application of actin depolymerizing drugs cytochalasin D and latrunculin A resulted in the simultaneous arrest of cytoplasmic streaming along the whole length of the pollen tube (Fig. 4 *B*).

The observed spatial gradient of the arrest of cytoplasmic streaming motivated us to verify whether the alterations in the actin cytoskeleton showed a similar spatial gradient along the longitudinal axis of challenged pollen tubes. The well defined chronology of SI-induced actin alterations (Geitmann et al., 2000) allowed us to identify the advancement of the response. Observations of pollen tubes having reached a length of several hundred micrometers at 10, 15,

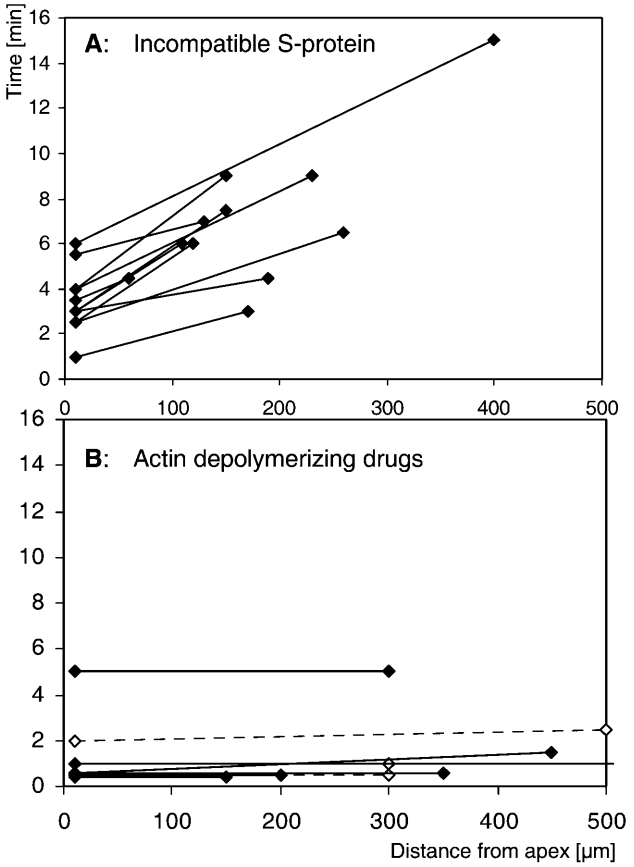

FIGURE 4 Arrest of cytoplasmic streaming does not occur simultaneously in all parts of the cell. (*A*) Treatment with incompatible S-protein. Time periods elapsed between SI challenge and complete arrest of cytoplasmic streaming in the apical and subapical versus the further distal areas are marked and connected for individual pollen tubes. The slopes indicate a spatial gradient. (*B*) Treatment with actin depolymerizing drugs. The graph shows the time periods elapsed between addition of cytochalasin D (*solid circles*) or latrunculin A (*open circles*) and complete arrest of cytoplasmic streaming in the apical and subapical versus the further distal areas of individual pollen tubes. The absence of significant slopes indicates that cytoplasmic streaming is affected simultaneously in all parts of one individual pollen tube.

and 20 min after SI induction revealed that the subapical and distal parts reacted differently within 10 min even though no significant structural differences were apparent between the thick actin bundles in the two regions. Whereas in the apical and subapical parts of long tubes actin had completely lost the F-actin bundled configuration and had transformed into punctate foci, distal parts of the same tube still showed remainders of filamentous structures at the same time point (Fig. 5). The application of actin depolymerizing drugs (1 μM cytochalasin D and 50 nM latrunculin A) showed that no differences in the susceptibility to actin depolymerizing activities between the subapical and distal parts of the cell existed, since disintegration of thick actin bundles occurred simultaneously in these regions (A. Geitmann, unpublished results).

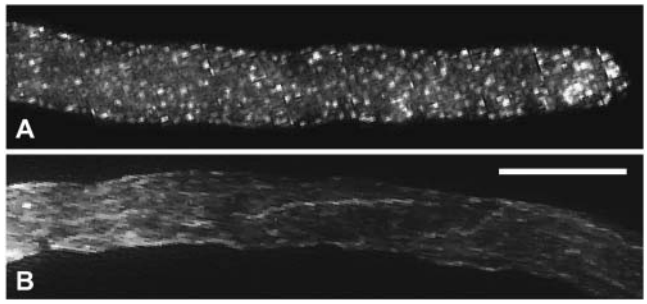

FIGURE 5 Actin is not rearranged at the same rate in all parts of the cell. Alexa 488-phalloidin label of different parts of two pollen tubes 15 min after SI challenge. Subapical actin bundles have disintegrated completely into punctate foci whereas distal actin bundles are still recognizable as such. Bar = 10 μm. (*A*) Apex; (*B*) distal part.

Localization of SI perception

The spatial gradient of the advancement of the SI responses in the form of arrest of cytoplasmic streaming and alteration of actin configuration, together with the absence of any obvious spatial gradient of actin filament stability along the longitudinal axis of the pollen tube, suggest that signal transduction and/or propagation occurs in a basipetal direction. This indicated that the pollen S-receptor may have an apical or subapical location. This was also suggested by previous observations of alterations in cytosolic free $[Ca^{2+}]$ (Franklin-Tong et al., 1993, 1997, 2002). To test whether we could provide corroborating evidence for the location of SI perception within the apex or subapical 100 μm of the pollen tube, we locally applied minute volumes of S-proteins to pollen tubes. This treatment, however, did not result in the SI response being elicited ($n = 7$). Higher concentrations of S-protein (400 μg/ml) resulted in an observable response in very few cases (3 out of 18), but only when S-proteins covered virtually the entire length of an individual pollen tube was it possible to consistently stimulate the S-specific arrest of pollen tube elongation.

DISCUSSION

Very few cytomechanical studies have been performed on living plant cells that have a reasonably thin cell wall which allows for intracellular changes in the physical behavior to become evident. Changes in turgor pressure have been the main cytomechanical feature that has been studied hitherto (Lintilhac et al., 2000, and references therein). Therefore, our approach is novel as it attempts to quantify the physical changes to the cytoplasm stimulated by a specific, defined ligand. This allowed us to demonstrate that in plant cells the rheological properties of the cytoplasm are subject to externally and internally triggered alterations.

Physical changes to the cytoplasm

Investigation of the physical behavior of *P. rhoeas* pollen tubes before and after SI induction, using mechanical

deformation and relaxation experiments revealed a considerable increase in the viscous component of the viscoelastic cellular behavior. A total arrest of organelle movement was also observed after SI. Both findings are consistent with the hypothesis that the viscosity of the cytoplasm increases after S-protein application. This increase in cytoplasmic viscosity can be described as a sol-gel transition, which is generally explained with chemical or physical reactions of molecules, polymers, or colloids. In cells this is often thought to be caused by an increase in actin filament density (Luby-Phelps, 2000; Fabry et al., 2001). However, this cannot be the case here, as we have previously shown that SI stimulates F-actin bundle disintegration (Geitmann et al., 2000) and actin filament depolymerization (Snowman et al., 2002).

Three other mechanisms that could be responsible for the sol-gel transition are

1. An increase in cytoplasmic density due to reduction in water content.
2. An increase of soluble substances in the cytoplasm, allowing the aggregation of previously freely diffusing molecules.
3. An increase in the degree of polymerization of cytoplasmic macromolecules, leading to formation of cross-links or entanglement of polymers.

Evidence consistent with the first hypothesis is provided by the observation that pollen tube stiffness decreases more than threefold after SI challenge. This is likely to be an effect of a decrease in turgor pressure (Lintilhac et al., 2000), which could account for higher cytoplasmic density. Signal-induced changes of turgor pressure are well-known phenomena that have been described in numerous plant and fungal cell types (Brownlee et al., 1998; Dixon et al., 1999; Findlay, 2001). In eukaryotic cells, turgor appears to be controlled by a conserved MAPK (mitogen-activated protein kinase) pathway (Brewster et al., 1993). Furthermore, Ca^{2+} is known to act as a second messenger in the turgor controlling signaling pathway involved in the tip growing *Fucus* rhizoid (Brownlee et al., 1998). This is consistent with the signals stimulated by SI.

It seems unlikely, however, that a simple decrease in turgor would be sufficient to cause the complete arrest of organelle oscillations that we observe in the SI response. The Brownian motion of a particle embedded within a filamentous network is directly related to the network's mechanical properties (Yamada et al., 2000, and references therein). Phenomenologically, particles exhibit larger motions when their local environments are less rigid or less viscous and vice versa. Organelle movement after breakdown of actin filaments is not dependent on molecular motors, so this should be an indicator for the mesh size of structural elements present in the cytoplasm. It is known that the cytoplasm is a rather concentrated solution, as the protein contents have been estimated at 200–300 g/L^{-1} for mammalian cells (Lanni et al., 1985). As a consequence, a change in water content is likely to cause a crowding effect, allowing or even driving self-assembly reactions of biomolecules (Luby-Phelps, 2000). The sustained increase of G-actin pool by depolymerization of F-actin observed in SI-challenged pollen tubes (Snowman et al., 2002) could potentially contribute to the crowding effect. The crowding could lead to polymerization or cross-linking events between macromolecules that might account for a change in rheology of the cytoplasm other than that caused by actin polymerization. In human lymphoblastoid cells undergoing apoptosis changes to cytoplasmic viscosity precede cell density changes, suggesting that structural changes in the cytoplasm can precede cell density changes (Dyson et al., 1986). This provides support for a turgor-independent mechanism and is consistent with the established model that regards the cytoplasm as able to undergo subcellular localized transitions between solvated, gelated, and contracted stages (Taylor and Fechheimer, 1982; Pollard, 1984; Porter, 1984; Luby-Phelps et al., 1986; Fabry et al., 2001).

A further fact that supports the cross-linking or formation of polymer entanglements hypothesis is the lack of disarrangement of polar organelle distribution after SI (this article and Franklin-Tong et al., 1993). In contrast, drug-induced actin depolymerization allowed bigger organelles to rapidly enter the apical clear zone. In tobacco pollen tubes these drugs seem to have similar effects, as can be deduced from a figure in Cheung et al. (2002). This phenomenon is consistent with a gel-sol transition of the cytoplasm to be expected upon disintegration of cytoskeletal elements. This suggests that as a result of the SI challenge, even though F-actin is depolymerized, some other structure prevents disruption of cell zonation. This, together with the observed increase in the viscous component of the cytoplasm upon SI suggests that a cross-linking, polymerization, or polymer entangling mechanism may be activated. Signal-induced cytoplasmic changes have hitherto mostly been attributed to alterations in the state of polymerization and cross-linking of cytoskeletal elements (Stossel, 1993; Wang et al., 1996, 1997; Lagaudriere et al., 1998). However, it is well known that other types of cellular macromolecules are subject to signal-induced cross-linking events, although these are located in the extracellular matrix, such as plant and yeast cell-wall polysaccharides (Levine et al., 1994; Kapteyn et al., 1997; Cazale et al., 1998), and matrix proteins such as elastin and collagen (Chithra et al., 1998; Smith-Mungo and Kagan, 1998; Velleman, 1999). Further studies are required to investigate the nature of the postulated cross-linking in the case of self-incompatible *Papaver* pollen tubes. In this context it will also be important to identify the role of the physical changes in the signaling process by identifying their precise development in time. The observation of the arrest of any cytoplasmic movement only minutes after SI challenge suggests that cytoplasmic viscosity might change early during the response, but the experimental set up of the micro-indentation experiments has prevented us from assessing the

physical properties of pollen tubes immediately after SI challenge. In either case, comparison with the time line of cellular events in the SI process reveals that the change in the physical property of the cytoplasm seems to take place during a period that is characterized by a number of protein phosphorylations (Franklin-Tong et al., 1993, 1997; Rudd and Franklin-Tong, 2003) and the rearrangement of the actin cytoskeleton (Geitmann et al., 2000, 2001; Snowman et al., 2002). On the other hand, it precedes the onset of structural and biochemical events that indicate the beginning of programmed cell death in the challenged pollen tube, such as organelle degeneration (starting 1 h after challenge), mitochondrial swelling (1–2 h), DNA fragmentation, and nuclear condensation (4 h) (Jordan et al., 2000; Rudd and Franklin-Tong, 2003; Geitmann et al., 2004). To identify the precise role of the viscosity changes in the signal transduction and response pathway, precise timing of the event will be of importance, but this approach requires the development of new experimental strategies.

Spatial propagation of the SI response in the subapical region

The putative pollen S-receptor has not been identified yet and therefore its precise cellular localization is unknown. However, a pollen transmembrane component is known to be required for the SI response, suggesting that the pollen S-receptor is located in the plasma membrane (Hearn et al., 1996). Hitherto only indirect evidence has existed for the site of signal perception. In SI-induced pollen tubes waves of increased $[Ca^{2+}]_i$ originate from an area 50–100 μm from the pollen tube apex (Franklin-Tong et al., 1993, 1997) and Ca^{2+} influx takes place in the same region (Franklin-Tong et al., 2002). Our observations on actin rearrangement and cytoplasmic streaming suggest that the SI signal may be perceived in the apical or subapical region. If the S-receptors were confined to this region, one would expect that a local application of the ligand would elicit a SI response. However, our results do not support this. Local application of S-proteins to confined regions of the pollen tube only rarely resulted in growth arrest unless virtually the entire pollen tube surface was in contact with the S-protein. The simplest explanation for this phenomenon is that the pollen S-receptors are not confined to a particular region and that a number of receptors need to be activated by the ligand to trigger the SI response. This result obviously raises questions about the in vivo situation. Further research is necessary to determine whether local contact of pollen tubes with an incompatible stigma is sufficient for SI induction. Furthermore, it remains to be shown why, in the in vitro-grown pollen tubes, the arrest of cytoplasmic streaming and alteration of actin configuration are more advanced in the subapical part of the cell compared to the distal areas. Whether it is the signal or the response that propagates along the tube, the fact that cytoplasmic streaming is arrested within a few minutes raises another intriguing question: Once long distance transport is halted, what is the mechanism of propagation of signal or response? In this context, studies on the spatial propagation of increases in $[Ca^{2+}]_i$ will be important.

In conclusion, our cytomechanical studies on the SI response in *P. rhoeas* pollen tubes have demonstrated that the physical properties of the cytoplasm undergo significant changes. To our knowledge, this represents the first time that cytoplasmic viscoelasticity has been studied in living plant cells. Alterations of the actin cytoskeleton and arrest of cytoplasmic streaming induced by the SI reaction are propagated in a basipetal direction in the tubular cell. However, an explanation for this phenomenon is still elusive, since our data do not support an exclusively apical location of the signal perception.

We thank Elliot Elson, Washington University, St. Louis, MO, for allowing us to perform the microindentation experiments in his laboratory.

A.G. was funded by a Marie Curie Postdoctoral Fellowship from the European Union. Work on microindentation was supported by grants from the Natural Sciences and Engineering Research Council of Canada and the Fonds Québecois de la Recherche sur la Nature et les Technologies to A.G.

REFERENCES

Baluska, F., P. Barlow, C. Staiger, and D. Volkmann. 2000. The Actin Cytoskeleton in Plant Cells. Kluwer Academic Publishers, Dordrecht, The Netherlands.

Brewster, J. L., T. de Valoir, N. D. Dwyer, E. Winter, and M. C. Gustin. 1993. An osmosensing signal transduction pathway in yeast. *Science*. 259:1760–1763.

Brownlee, C., N. F. H. Manison, and R. Anning. 1998. Calcium, polarity and osmoregulation in *Fucus* embryos: one messenger, multiple messages. *Exper. Biol. On-line*. 3.

Cazale, A.-C., M.-A. Rouet-Mayer, H. Barbier-Brygoo, and Y. Mathieu. 1998. Oxidative burst and hypoosmotic stress in tobacco cell suspensions. *Plant Physiol.* 116:659–669.

Cheung, A. Y., C. Y. Chen, R. H. Glaven, B. H. de Graaf, L. Vidali, P. K. Hepler, and H. M. Wu. 2002. Rab_2 GTPase regulates vesicle trafficking between the endoplasmic reticulum and the Golgi bodies and is important to pollen tube growth. *Plant Cell.* 14:945–962.

Chithra, P., G. B. Sajithlal, and G. Chandrakasan. 1998. Influence of aloe vera on collagen characteristics in healing dermal wounds in rats. *Mol. Cell. Biochem.* 181:71–76.

Dixon, K. P., J. R. Xu, N. Smirnoff, and N. J. Talbot. 1999. Independent signaling pathways regulate cellular turgor during hyperosmotic stress and *appressorium*-mediated plant infection by *Magnaporthe grisea*. *Plant Cell.* 11:2045–2058.

Dyson, J. E. D., D. M. Simmons, J. Daniel, J. M. McLaughlin, P. Quirke, and C. C. Bird. 1986. Kinetic and physical studies of cell death induced by chemotherapeutic agents or hyperthermia. *Cell Tissue Kin.* 19:311–324.

Elson, E. L., B. B. Daily, W. B. McConnaughey, C. Pasternak, and N. O. Petersen. 1983. Measurement of forces which determine the shapes of adherent cells in culture. *In* Frontiers in Biochemical and Biophysical Studies of Proteins and Membranes. T.-Y. Liu, S. Sakakibara, A. Schechter, K. Yagi, H. Yajima, and K. T. Yasunobu, editors. Elsevier, New York. 399–411.

Esseling, J. J., F. G. P. Lhuissier, and A. M. C. Emons. 2003. Nod factor-induced root hair curling: continuous polar growth towards the point of Nod factor application. *Plant Physiol.* 132:1982–1988.

Evans, E. A., and A. Yeung. 1989. Apparent viscosity and cortical tension of blood granulocytes determined by micropipet aspiration. *Biophys. J.* 56:151–160.

Fabry, B., G. N. Maksym, J. P. Butler, M. Glogauer, D. Navajas, and J. J. Fredberg. 2001. Scaling the microrheology of living cells. *Phys. Rev. Lett.* 87:148102/1–4.

Findlay, G. P. 2001. Membranes and the electrophysiology of turgor regulation. *Austral. J. Plant Physiol.* 28:617–634.

Foote, H. G., J. P. Ride, V. E. Franklin-Tong, E. A. Walker, M. J. Lawrence, and F. C. H. Franklin. 1994. Cloning and expression of a novel self-incompatibility (*S*-)gene from *Papaver rhoeas*. *Proc. Natl. Acad. Sci. USA.* 91:2265–2269.

Franklin-Tong, V. E., G. Hackett, and P. K. Hepler. 1997. Ratio-imaging of $[Ca^{2+}]_i$ in the self-incompatibility response in pollen tubes of *Papaver rhoeas*. *Plant J.* 12:1375–1386.

Franklin-Tong, V. E., T. L. Holdaway-Clarke, K. R. Straatman, J. G. Kunkel, and P. K. Hepler. 2002. Involvement of extracellular calcium influx in the self-incompatibility response of *Papaver rhoeas*. *Plant J.* 29:333–345.

Franklin-Tong, V. E., M. J. Lawrence, and F. C. H. Franklin. 1988. An in-vitro method for the expression of self-incompatibility in *Papaver rhoeas* using stigmatic extracts. *New Phytol.* 110:109–118.

Franklin-Tong, V. E., J. P. Ride, and F. C. H. Franklin. 1995. Recombinant stigmatic self-incompatibility (S-) protein elicits a Ca^{2+} transient in pollen of *Papaver rhoeas*. *Plant J.* 8:299–307.

Franklin-Tong, V. E., J. P. Ride, N. D. Read, A. J. Trewavas, and F. C. H. Franklin. 1993. The self-incompatibility response in *Papaver rhoeas* is mediated by cytosolic free calcium. *Plant J.* 4:163–177.

Geitmann, A., V. E. Franklin-Tong, and A. M. C. Emons. 2001. Early cellular events in pollen tubes during the self-incompatibility reaction. *In* Cell Biology of Plant and Fungal Tip Growth. A. Geitmann, M. Cresti, and I. E. Heath, editors. IOS Press, Amsterdam. 203–219.

Geitmann, A., V. E. Franklin-Tong, and A. M. C. Emons. 2004. The self-incompatibility response in *Papaver rhoeas* pollen causes early and striking alterations to organelles. *Cell Death Differentiation.* In press.

Geitmann, A., and E. Parre. 2004. The local cytomechanical properties of growing pollen tubes correspond to the axial distribution of structural cellular elements. *Sexual Plant Reprod.* 17. In press.

Geitmann, A., B. Snowman, V. E. Franklin-Tong, and A. M. C. Emons. 2000. Alterations in the actin cytoskeleton of the pollen tube are induced by the self-incompatibility reaction in *Papaver rhoeas*. *Plant Cell.* 12:1239–1251.

Hearn, M. J., F. C. H. Franklin, and J. P. Ride. 1996. Identification of a membrane glycoprotein in pollen of *Papaver rhoeas* which binds stigmatic self-incompatibility (S-)proteins. *Plant J.* 9:467–475.

Heslop-Harrison, J. 1987. Pollen germination and pollen-tube growth. *Int. Rev. Cytol.* 107:1–78.

Ingber, D. E. 1993. Cellular tensegrity: defining new rules of biological design that govern the cytoskeleton. *J. Cell Sci.* 104:613–627.

Jordan, N. D., F. C. H. Franklin, and V. E. Franklin-Tong. 2000. Evidence for DNA fragmentation triggered in the self-incompatibility response in pollen of *Papaver rhoeas*. *Plant J.* 23:471–479.

Kakeda, K., N. D. Jordan, A. Conner, J. P. Ride, V. E. Franklin-Tong, and F. C. H. Franklin. 1998. Identification of residues in a hydrophilic loop of the *Papaver rhoeas* S-protein that play a crucial role in recognition of incompatible pollen. *Plant Cell.* 10:1723–1731.

Kapteyn, J. C., A. F. J. Ram, E. M. Groos, R. Kollar, R. C. Montijn, H. Van Den Ende, A. Llobell, E. Cabib, and F. M. Klis. 1997. Altered extent of cross-linking of β-1,6-glucosylated mannoproteins to chitin in *Saccharomyces cerevisiae* mutants with reduced cell wall β-1,3-glucan content. *J. Bacteriol.* 179:6279–6284.

Lagaudriere, G. C., S. Lebel-Binay, C. Hubeau, D. Fradelizi, and H. Conjeaud. 1998. Signaling through the tetraspanin CD82 triggers its association with the cytoskeleton leading to sustained morphological changes and T cell activation. *Eur. J. Immunol.* 28:4332–4344.

Lanni, F., A. S. Waggoner, and D. L. Taylor. 1985. Structural organization of interphase 3T3 fibroblasts studied by total internal reflection fluorescence microscopy. *J. Cell Biol.* 100:1091–1102.

Levine, A., R. Tenhaken, R. Dixon, and C. Lamb. 1994. H_2O_2 from the oxidative burst orchestrates the plant hypersensitive disease. *Cell.* 79: 583–593.

Lintilhac, P. M., C. Wei, J. J. Tanguay, and J. O. Outwater. 2000. Ball tonometry: a rapid, nondestructive method for measuring cell turgor pressure in thin-walled plant cells. *J. Plant Growth Reg.* 19:90–97.

Loitto, V. M., B. Rasmusson, and K. E. Magnusson. 2001. Assessment of neutrophil *n*-formyl peptide receptors by using antibodies and fluorescent peptides. *J. Leukoc. Biol.* 69:762–771.

Luby-Phelps, K. 2000. Cytoarchitecture and physical properties of cytoplasm: volume, viscosity, diffusion, intracellular surface area. *Int. Rev. Cytol.* 192:189–221.

Luby-Phelps, K., D. L. Taylor, and F. Lanni. 1986. Probing the structure of cytoplasm. *J. Cell Biol.* 102:2015–2022.

Palanivelu, R., and D. Preuss. 2000. Pollen tube targeting and axon guidance: parallels in tip growth mechanisms. *Trends Cell Biol.* 10:517–524.

Petersen, N. O., W. B. McConnaughey, and E. L. Elson. 1982. Dependence of locally measured cellular deformability on position on the cell, temperature, and cytochalasin B. *Proc. Natl. Acad. Sci. USA.* 79:5327–5331.

Pollard, T. D. 1984. Molecular architecture of the cytoplasmic matrix. *In* White Cell Mechanics: Basic Science and Clinical Aspects. H. J. Meiselman, M. A. Lichtman, and P. L. LaCelle, editors. Alan R. Liss, New York. 75–86.

Porter, K. R. 1984. The cytomatrix: a short history of its study. *J. Cell Biol.* 99:3s–12s.

Rudd, J. J., and V. E. Franklin-Tong. 2001. Unravelling response-specificity in Ca^{2+} signalling pathways in plant cells. *New Phytol.* 151:7–34.

Rudd, J. J., and V. E. Franklin-Tong. 2003. Signals and targets of the self-incompatibility response in pollen of *Papaver rhoeas*. *J. Exper. Bot.* 54:141–148.

Schmid-Schoenbein, G. W., T. Kosawada, R. Skalak, and S. Chien. 1995. *ASME J. Biomech. Eng.* 117:171–178.

Smith-Mungo, L. I., and H. M. Kagan. 1998. Lysyl oxidase: properties, regulation and multiple functions in biology. *Matrix Biol.* 16:387–398.

Snowman, B. N., D. R. Kovar, G. Shevchenko, V. E. Franklin-Tong, and C. J. Staiger. 2002. Signal-mediated depolymerization of actin in pollen during the self-incompatibility response. *Plant Cell.* 14:2613–2626.

Stamenovic, D., and M. F. Coughlin. 1999. The role of prestress and architecture of the cytoskeleton and deformability of cytoskeletal filaments in mechanics of adherent cells: a quantitative analysis. *J. Theor. Biol.* 201:63–74.

Stamenovic, D., J. J. Fredberg, N. Wang, J. P. Butler, and D. E. Ingber. 1996. A microstructural approach to cytoskeletal mechanics based on tensegrity. *J. Theor. Biol.* 181:125–136.

Stossel, T. P. 1993. On the crawling of animal cells. *Science.* 260:1086–1094.

Strutt, D. I. 2001. Asymmetric localization of Frizzled and the establishment of cell polarity in the *Drosophila* wing. *Mol. Cell.* 7:367–375.

Taylor, D. L., and M. Fechheimer. 1982. Cytoplasmic structure and contractility: the solvation-contraction coupling hypothesis. *Philos. Trans. R. Soc. Lond. B Biol. Sci.* 299:185–187.

Vantard, M., and L. Blanchoin. 2002. Actin polymerization processes in plant cells. *Curr. Opin. Plant Biol.* 5:502–506.

Velleman, S. G. 1999. The role of the extracellular matrix in skeletal muscle development. *Poult. Sci.* 78:778–784.

Vidali, L., and P. K. Hepler. 2001. Actin and pollen tube growth. *Protoplasma*. 215:64–76.

Wang, N., K. Naruse, D. Stamenovic, J. J. Fredberg, S. M. Mijailovich, I. M. Tolic-Nørrelykke, T. Polte, R. Mannix, and D. E. Ingber. 2001. Mechanical behavior in living cells consistent with the tensegrity model. *Proc. Natl. Acad. Sci. USA*. 98:7765–7770.

Wang, Q., W. F. Patton, E. T. Chiang, H. B. Hechtman, and D. Shepro. 1996. Filamin translocation is an early endothelial cell inflammatory response to bradykinin: regulation by calcium, protein kinases, and protein phosphatases. *J. Cell. Biochem.* 62:383–396.

Wang, Q., W. F. Patton, H. B. Hechtman, and D. Shepro. 1997. A novel anti-inflammatory peptide inhibits endothelial cell cytoskeletal rearrangement, nitric oxide synthase translocation, and paracellular permeability increases. *J. Cell. Physiol.* 172:171–182.

Wheeler, M. J., V. E. Franklin-Tong, and F. C. H. Franklin. 2001. The molecular and genetic basis of pollen-pistil interactions. *New Phytol.* 151:565–584.

Yamada, S., D. Wirtz, and S. C. Kuo. 2000. Mechanics of living cells measured by laser tracking microrheology. *Biophys. J.* 78:1736–1747.